JKAU: Mar. Sci., **Vol. 19**, pp: 61-74 (2008 A.D. / 1429 A.H.)

Temporal and Spatial Variations of Remotely Sensed Sea Surface Temperature in the Northern Red Sea

Abdullah M. Al-Subhi and **Moussa M. Al-Aqsum**

Faculty of Marine Science,
King Abdulaziz University, Jeddah, Saudi Arabia
amalsubhi@kau.edu.sa

Abstract. The present study shows the reliability of satellite data, when the monthly averages of satellite derived SST in the northern half of the Red Sea from January 1996 to December 2003 from AVHRR-SST imageries are compared with sea surface temperature data from previous studies. The pronounced monthly fluctuations of SST were observed. Higher SST is in the southeast and east on the Saudi side of the Red Sea, while the lower SST is on the African side. The SST fluctuations are mainly correlated with the air temperature, wind speed and heat loss due to evaporation. A multiple regression model for the SST fluctuations is proposed that explains the observed SST. Power spectrum of the SST showed that in the northern Red Sea the annual cycle of temperature change is dominant. The comparatively warm period of (1997-1999) may be due to the El Niño effect and, the lower SST of period (2000-2003) may be La Niña cycle and/or due to the 11-year cycle of sunspot activities. However, all these assumptions need further investigations.

Introduction

The interest in the remote sensing of the ocean parameters has grown because of its capability to get data over a large area at the same time which otherwise is not possible by conventional methods. Sea surface temperatures (SST) variations are an important indicator of the climate changes as well as a key factor in the coupling between the atmosphere and the ocean. SST variations in the ocean occur in response to surface heat fluxes at the air-sea interface and the horizontal and vertical heat transfer within the ocean itself. Therefore, it is very important to

understand SST behavior on a large scale. SST variations in the Red Sea (Fig. 1) are affected by a number of factors such as excess evaporation over precipitation, air temperature, and reversal of wind regime and the associated current patterns, land and topographic effects and daily and seasonal weather changes. Morcos (1970) has summarized previous studies regarding horizontal distribution of surface temperature and SST variations in the northern half of the Red Sea. The temperature decreases from south to north and from east to west. Also higher temperature is to the southeast and east on the Arabian side of the sea, while the lower temperature is on the African side. Towards the north of the Red Sea the surface water becomes denser due to cooling by evaporation and the latitudinal decrease of temperature. As a result, it sinks to the deep layer and then it flows towards the south.

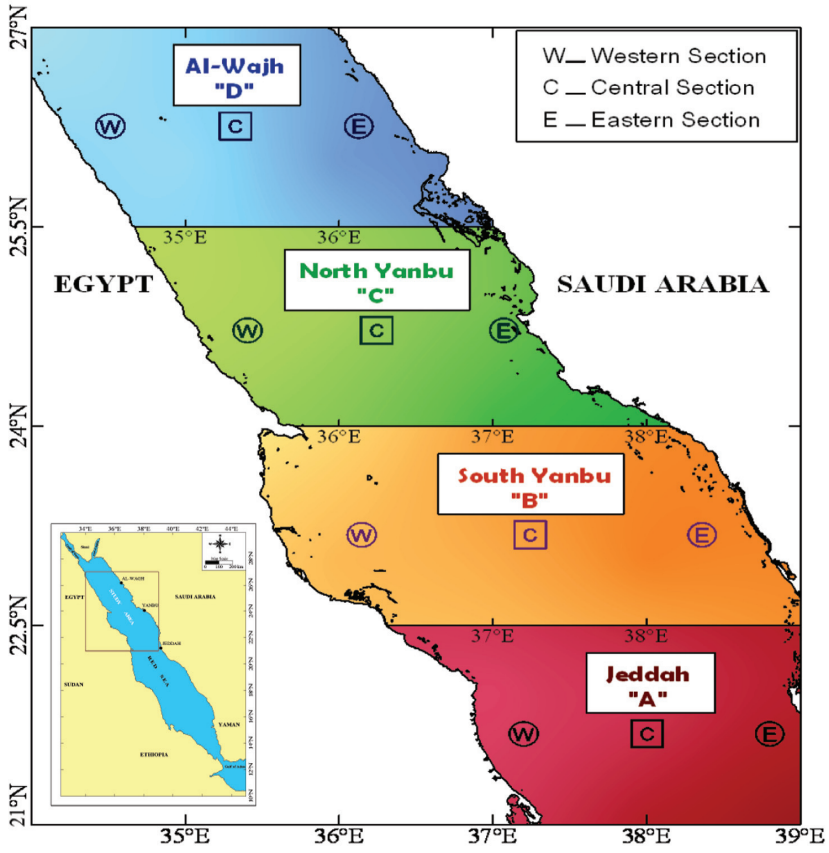

Fig. 1. Map of the study area showing the sections for latitudinal regions of Jeddah, south Yanbu, north Yanbu, and Al-Wajh.

Al-Barakati *et al.* (2002) showed that the surface temperature decreases more regularly from south to north in the northern Red Sea. Sultan and Ahmed (1991) performed spectral analysis on the monthly mean sea surface temperature data near Jeddah and showed a dominant annual cycle. Both thermohaline forcing and wind are responsible for generating circulation in the Red Sea (Morcos, 1970; and Wassef *et al*., 1983). In the early summer the winds are less uniform (Patzert, 1974) and it is generally admitted that the main driving force is buoyancy (Maillard and Soliman, 1986).

The objective of the present study is to use the SST images data set acquired by the Advanced Very High Resolution Radiometer (AVHRR), on board the National Oceanic and Atmospheric Administration (NOAA) series polar-orbiting operational environmental satellite, to investigate the horizontal variations of SST temporal and spatial variability over the northern half of the Red Sea (21°-27° N and 34°-39° E) (Fig. 1), by applying the methods of time series analysis.

Data and Methods of Analysis

The study area was segmented to four regions for time series analysis. The images data were then divided to four regions from south to north. Each region is spaced at 1.5° latitudinal interval; Jeddah region (A), south Yanbu region (B), North Yanbu (C), and Al-Wajh region (D). Each region was divided into three sections which include; Western (W), Central (C), and Eastern (E) sections. Therefore in all, 12 sections are considered for the statistical analysis of SST (Fig. 1).

Satellite-Derived SST Data Set

Sea surface temperature (SST) data derived from NOAA/AVHRR through the night-time multi-channel SST (MCSST) data set, obtained by the National Aeronautics and Space Administration (NASA). Physical Oceanography Distributed Active Archive Centre (PO.DAAC) at the Jet Propulsion Laboratory (JPL) are available on (URL: http://poet.-jpl.nasa.gov). The SST images data for this study are from January 1996 to December 2003, provided as a monthly averages data set with an accuracy of 0.3°C and a higher spatial resolution of 4 km. The AVHRR instrument has three infrared (IR) channels, [**ch3**, 3.55–3.93 μm; **ch.4**,

10.3–11.3 μm; **ch.5**, 11.5–12.5 μm], which are capable of measuring the SST (Reynolds and Smith, 1994; and Walton *et al*., 1998).

The monthly mean satellite data, in a grid of 0.043945° × 0.043945° pixel covering the northern half of the Red Sea, were remapped to a Geographical projection at 21°N to 27°N and 34°E to 39°E. Each data file (96 months) includes monthly averages of SST for both the land and sea values. The filtered data (grid-points of land are removed) covers the sea in each monthly average data file. Some data sets had large missing values at some locations of study area because of clouds, which created a difficulty in investigating the data. This problem was solved by averaging all non-cloud pixels array centered on each grid point, constructing a time series at each grid point. Then, data were reduced to 100 grids (Fig. 2) to remove errors from data values because of missing numbers. Also, the grid-points locations should be away from shore line. The SST data are in the form of digital numbers (DN). From the digital number (DN) the SST in degrees Celsius (°C) was obtained by using the following equation:

$$SST = 0.075 \times DN - 0.3$$

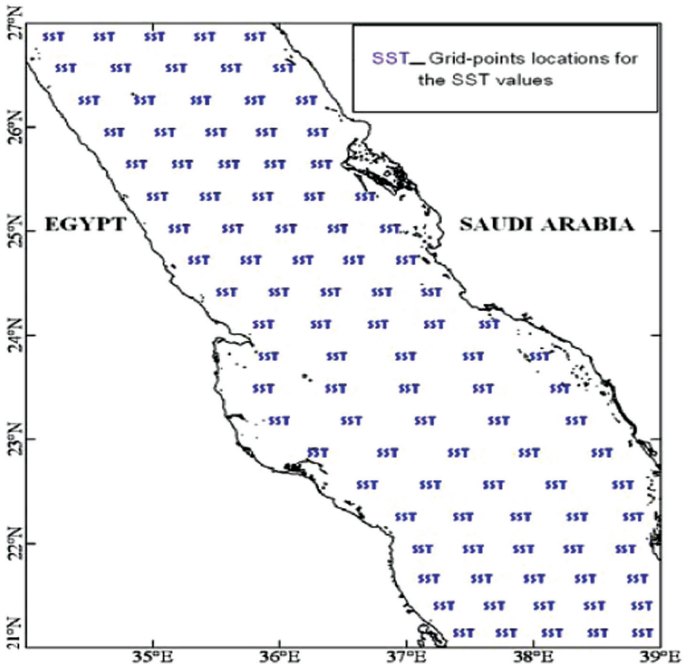

Fig. 2. Map of the study area showing the grid-points locations for the SST values of the reduced data of (5 × 20) grid-points.

Where;

SST : Sea Surface Temperature (degrees Celsius).

DN : Digital Number.

Then the temporal variations of SST for monthly averages from AVHRR data were computed to understand the mechanism of changes in patterns of SST through the months and years in the study area. Figure 3 shows the monthly average of SST (average of all grid points) for the study area as a whole from Jan. 1996 to Dec. 2003.

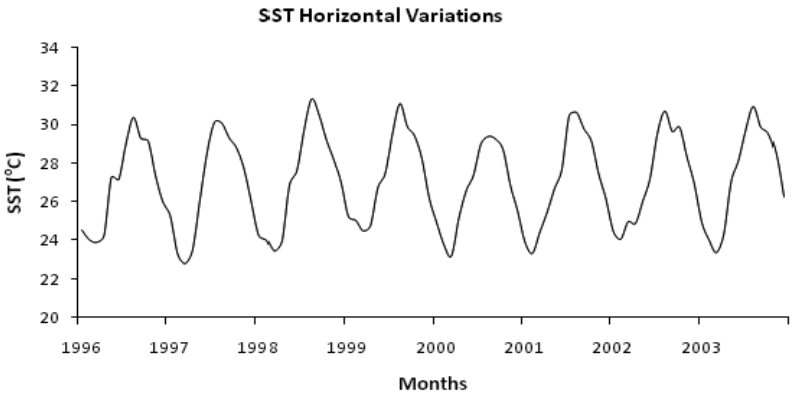

Fig. 3. The monthly average (1996-2003) of SST based on AVHRR images data for the study area (21°-27° N, 34°-39°E).

Figure 4 gives the monthly average for all the sections (averaged for the grid points in a section for a month and the Averaged for that particular month from 1996-2003, *e.g.* April month is average of all Aprils from 1996-2003).

Figure 5 gives the monthly averages of SST variations for the central regions of Jeddah, South Yanbu, North Yanbu, and Al-Wajh.

Time Series Analysis

The SST analysis is carried out using statistically based time series methods, described by Chatfield (1989) which include: (a) Calculating linear trend by applying the linear regression technique and then removing trend component from SST time series, (b) seasonal component is also calculated and removed from SST data, (c) power

spectral analysis employing FFT techniques to study the annual and semi-annual cycles of SST time series, and (d) polynomial analysis was used for the detrended, deseasonalized data to calculate the cycle of SST time series for all central sections. Figure 6 (a to d) show the residual SST fluctuations of central sections for Jeddah, Yanbu, and Al-Wajh (after removing trend and seasonality).

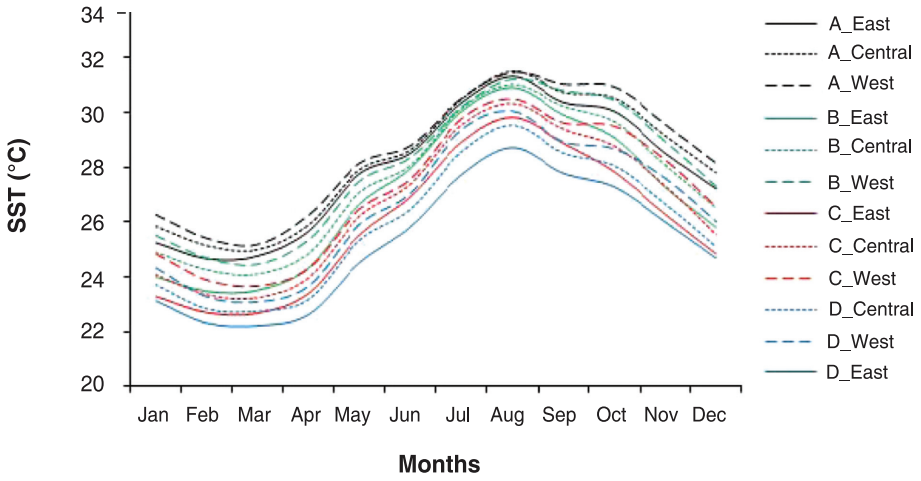

Fig. 4. The monthly average (1996-2003) of SST based on AVHRR images data for a) Jeddah, b) south Yanbu, c) north Yanbu, and d) Al-Wajh regions.

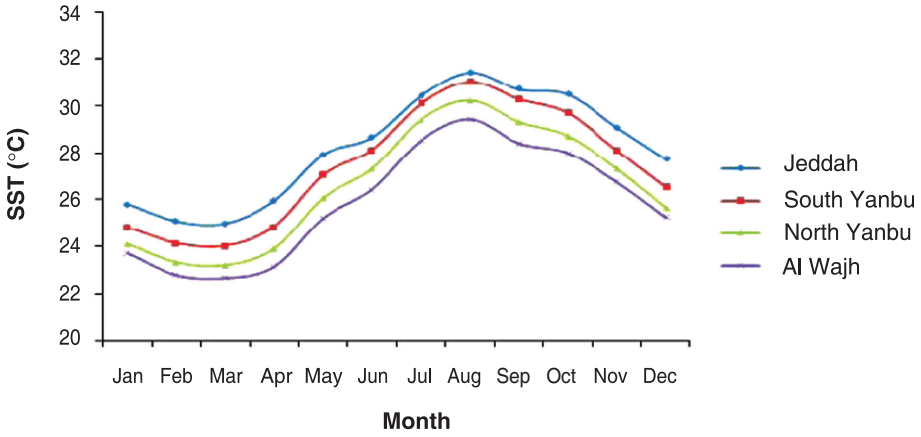

Fig. 5. The monthly variations of SST in northern Red Sea sections (averaged).

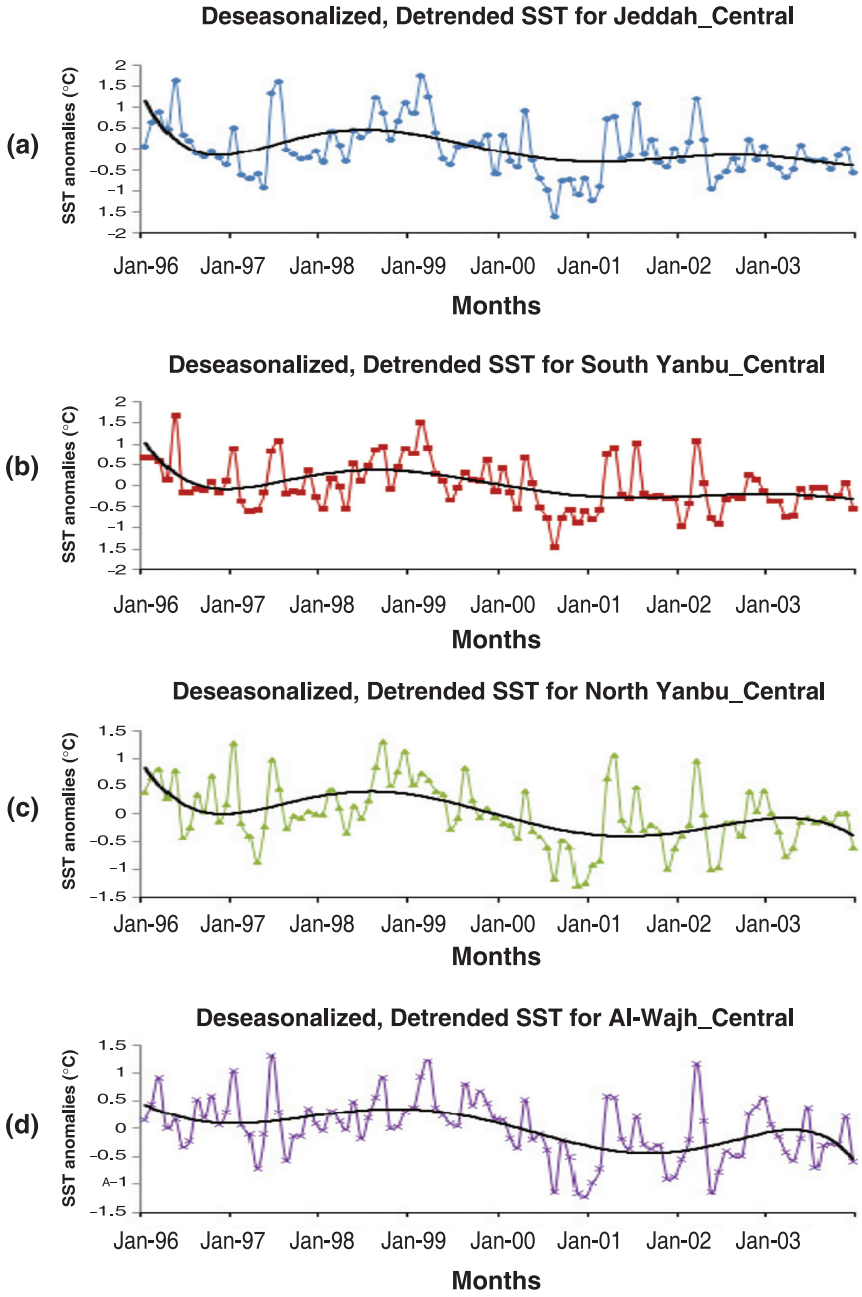

Fig. 6(a-d). The monthly variations (1996-2003) of SST at the central sections after removing trend and seasonality for a) Jeddah, b) south Yanbu, c) north Yanbu, and d) Al-Wajh regions. Bold black lines indicate SST cycles in all regions.

Anomalies computed with respect to central sections show major SST anomalies, such as warm or cool episodes in the northern half of the Red Sea. The inter-annual cycles of the residual SST for all central sections, show that the phase and amplitude of each is roughly the same. Applying the polynomial trend on the residual SST data shows clearly a 3-4 years cycle of SST variations in northern half of the Red Sea for all regions (Fig. 6: a to d). The cycle for the central sections shows a comparatively warm period of (1997-1999) and lower SST during (2000-2003). The warm period may be due to the El Niño effect and the period (2000-2003) may be associated with La Niña cycle. However, there is a probability that these periods are associated with the 11-year cycle of sunspot activities

Fast Fourier Transform (FFT)

The result of the power spectra of the SST variations are presented in Fig. 7 (a to d) for the four central sections for Jeddah, south Yanbu, north Yanbu, and Al-Wajh regions. The SST presents high coherence over almost the whole range of frequencies in the spectrum. The dominant peak is located at a band of period around twelve month (*i.e.* the annual cycle) for four regions. Therefore, the most energetic component is the annual cycle for four regions in the northern half of the Red Sea.

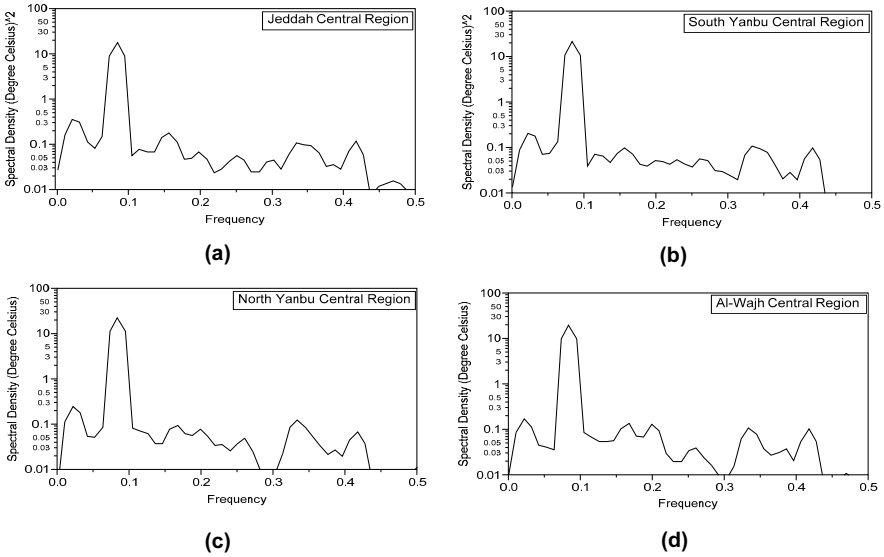

Fig. 7(a-d). The power spectrum density of SST at the central sections for a) Jeddah, b) south Yanbu, c) north Yanbu, and d) Al-Wajh regions.

Meteorological Parameters and Observed Sea Surface Temperature Data

Monthly averages (1996-2003) of observed sea surface temperature (Ts) were taken from National Oceanographic Data Center (NODC) available on (www.nodc.noaa.gov). These monthly averages of sea surface temperature are for three coastal stations Jeddah, Yanbu, Al-Wajh along the northern Red Sea located at about 21°N, 39°25'E; 24.1°N, 38°E; and 26.2°N, 36.5°E, respectively. In addition, monthly averages of meteorological data including air temperature (Ta), wind speed (Ws) and relative humidity (Rh) were provided by Presidency of Meteorology and Environment (PME) of Saudi Arabia for a period of 8 years (1996-2003) at three coastal stations, Jeddah, Yanbu, Al-Wajh along the northern Red Sea located at about (21°42'37"N, 39°11'12"E), (24°08'24"N, 38°03'50"E) and (26°12'19"N, 36°28'37"E) respectively. The meteorological data sites are fairly representative of the northern Red Sea. Using sea surface temperature, air temperature, wind speed, and humidity, the evaporative heat flux (Ws) was estimated using bulk aerodynamic method, according to Ahmad *et al*., (1989). The three locations are fairly spread along the northern Red Sea and the averages of the heat fluxes at these locations will be representative of the northern Red Sea as a whole. The plots of observed sea surface temperature, air temperature, wind speed, and evaporation heat flux for Jeddah, Yanbu, and Al-Wajh regions are given in Fig. 8 (a to d) respectively.

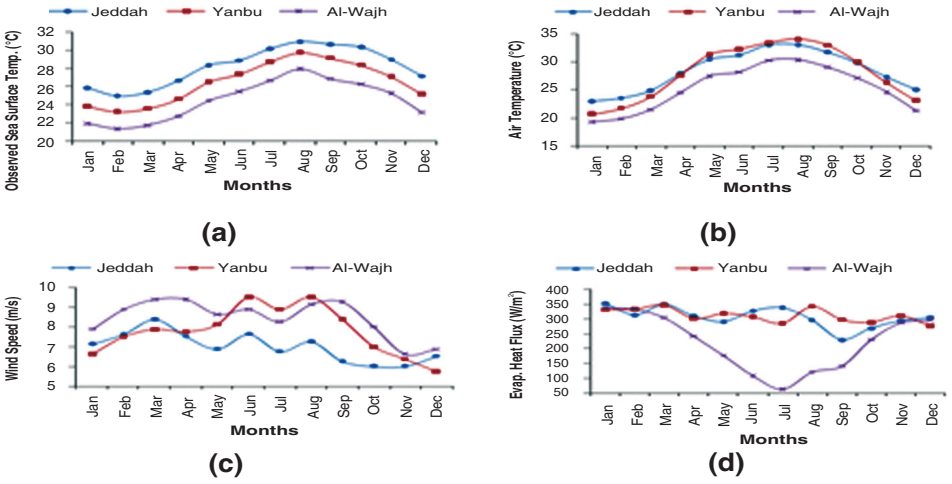

Fig. 8. The monthly variations of a) observed sea surface temperautre (*Ts*) in °C, b) air temperaure (*Ta*) in °C, c) wind speed (*Ws*) in m/s, and d) evaporative heat flux (Q_e) in w/m^2.

Results and Discussion

Figure 3 shows the monthly averages of SST for the study area as a whole from Jan 1996 to Dec 2003. The SST diagram shows higher SST in 1998, 1999, and 2003 and lower in 2000. The monthly averages of SST for 12 regions are given in Fig. 4 and the monthly variations of SST for central sections of the four regions are given in Fig. 5. It can be seen from Fig. 4 that generally SST is higher on the western side and lower on the eastern side. The SST increases from north to south (Fig. 5), and from west to east at the same latitude (*i.e.* the temperature on the eastern side is higher than that on the western side). Higher SST in the southeast and east on the Saudi side of the sea, may be due to movement of the air to the east which becomes more humid so the rate of evaporation from the sea surface decreases and hence the sea surface temperature will increase, while the lower temperature on the African side is due to less humid air and consequently high evaporation. In the north of the Red Sea the water becomes denser, and will sink to the lower layer and then will flow toward the south to form the outflow water.

Forecasting Model

Linear multiple regression models including autocorrelation terms were used to forecast the SST in the four central sections of the study area. Calculations were made with 95% confidence intervals. Standard (Pearson) correlation technique was used to find dominant factors controlling the SST of central sections. Based on the regression coefficients, the SST is computed for the four central sections of the regions. Examining a number of possible causes, sea surface temperature fluctuations are explained mostly by the air temperature, wind and evaporative heat flux. A multiple regression model that explains 95% of the SST fluctuations is proposed that explains the observed SST for all central sections. Results give the following fitted model for the monthly average of the SST for four regions;

$$y_{\text{Jed}} = 24.785 - 2.860\ W_s + 0.456\ T_a + 0.005\ Q_e$$

$$y_{\text{S.Y}} = 14.479 - 2.269\ W_s + 0.657\ T_a + 0.022\ Q_e$$

$$y_{\text{N.Y}} = 13.206 - 2.179\ W_s + 0.663\ T_a + 0.022\ Q_e$$

$$y_{\text{Wjh}} = 20.431 - 2.172\ W_s + 0.603\ T_a + 0.002\ Q_e$$

where;

$y_{\text{Jed}}, y_{\text{S.Y}}, y_{\text{N.Y}}, y_{\text{Wjh}}$ are the computed SST (SSTc) in (°C) for four central regions Jeddah, south Yanbu, north Yanbu, and Al-Wajh, respectively.

W_s = the wind speed (m/sec).

T_a = the air temperature (°C).

Q_e = the evaporative heat flux (w/m^2).

The coefficients of estimates with their standard error and the 95% confidence intervals are given in Table 1. The fitted model was compared with the observed monthly sea surface temperature in Fig. 9 (a to d) and indicates a good agreement with the SST patterns at four central regions (Jeddah, south Yanbu, north Yanbu, and Al-Wajh). Each controlling factor is discussed separately to study their effects on the SST fluctuations in the study area.

Table 1. The correlation coefficients for the central section between the SST and the main significant factors for Jeddah, south Yanbu, north Yanbu, and Al-Wajh regions.

Significant factors	Jeddah central	S. Yanbu central	N. Yanbu central	Al-Wajh central
	Pearson correlations			
Wind Speed (W_s)	–0.646	0.442	0.459	–0.112
Air Temperature (T_a)	0.840	0.841	0.846	0.857
Evaporative Heat Flux (Q_e)	–0.583	–0.368	– 0.357	–0.760

a. Air Temperature and Sea Surface Temperature

Air temperature differences play a significant role in the SST variability. The relation between air temperature and the sea surface temperature is linear, both decreasing northward. The air temperature normally has the lower value over the northern part of the Red Sea all the year. The northern part of the sea is subjected to greater variability of weather than the south, particularly in winter when it may be influenced by disturbances in the Mediterranean. However from May to September the air temperature at Yanbu is somewhat higher compared to that at Jeddah. The SST has a positive correlation with the air temperature in all the regions and is about 0.9 throughout the year.

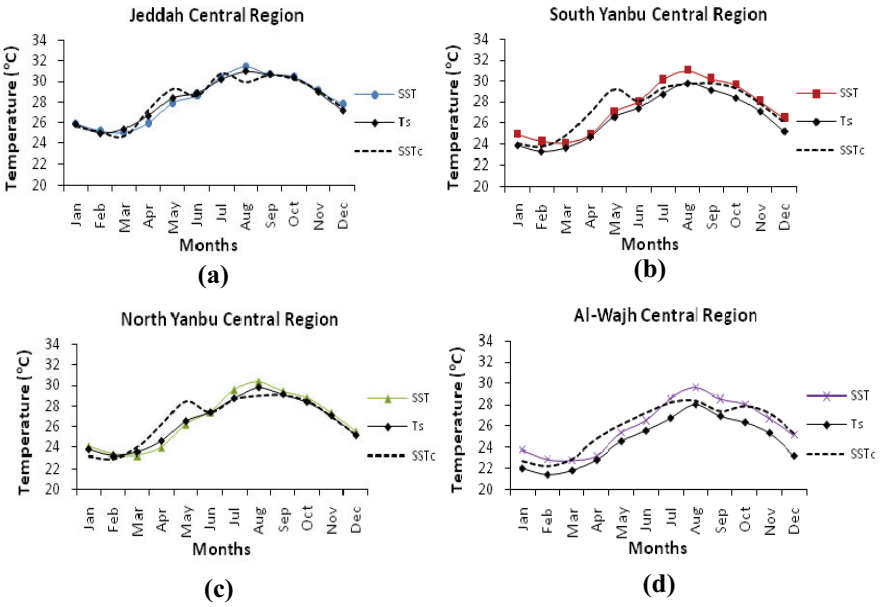

Fig. 9(a-d). The monthly averages SST measured from AVHRR images, T_s from NODC and computed mean SSTc based on the multiple-regression model for a) Jeddah, b) south Yanbu, c) north Yanbu, and d) Al-Wajh regions.

b. Wind Effect

The wind field over the northern Red Sea shows that the prevailing winds blow from a window north-northwest during the whole year. The effect of the wind speed is important for the SST variability causing decrease or increase in SST. The effect of the wind field on the SST variability has been examined and shows a correlation of about 0.5 in Yanbu regions. It can be seen that the general pattern of the wind field is the important component of the seasonal variability of SST.

c. Evaporation

Evaporative heat flux results in lowering the SST. Monthly averages of the SST show maximum depression during winter associated with the higher rates of evaporative heat flux. Therefore, SST at Al-Wajh region is highly correlated with the loss of heat by evaporation. During the winter, the horizontal fluxes are increasing northward due to the loss of water by evaporative heat flux. The relationship between SST and evaporative heat flux differs at each section. The close correlation of the

SST and evaporative heat flux are noticeable in the Al-Wajh and Jeddah regions.

A correlation coefficient between the main significant controlling factors and the horizontal SST computed from the nighttime MCSSTs for all seasons shows that the main significant controlling factors for the SST has a statistically significant correlations in every region. The first comparison using the Pearson Correlation coefficients technique shows that wind speed, air temperature, and evaporative heat flux display correlation with the SST fluctuation.

Acknowledgements

Dr. Fazal Ahmad is thanked for his suggestions in preparing this manuscript. Presidency of Meteorology and Environment (PME) is thanked for providing meteorological data. Images data with the global MCSST data set were provided by PO.DAAC (the Physical Oceanography Distributed Active Archive Center), and are available at URL: http://poet.jpl.nasa.gov/.

References

Ahmad, F., **Sultan, S.A.R.** and **Moammar M.O.** (1989) Monthly variations of net heat flux at the air-sea interface in coastal waters near Jeddah Red Sea, *Atmosphere Ocean*, **27**(2): 406-415.

Al-Barakati, A.M.A., James, A.E. and **Karakes, G.M.** (2002) A three dimensional hydrodyamical model to predict the distribution of temperature, salinity and water circulation of the Red Sea, *JKAU: Mar. Sci.*, **13**: 3-16.

Chatfied, C. (1989) *The Analysis of Time Series: An Introduction*, London: Chapman and Hall, 241 p.

Maillard, C. and **Soliman, G.** (1986) Hydrography of the Red Sea and exchanges with the Indian ocean in summer, *Oceanologica Acta*, **9**(3): 249-269.

Morcos, S.A. (1970) Physical and chemical oceanography of the Red Sea, *Oceanography and Marine Biology Annual Review*, **8**: 73-202.

Reynolds, R.W. and **Smith**, **T.M.** (1994) Improved global sea surface temperature analyses, *J. Climate*, **7:** 929-948.

Sultan, S.A.R. and **Ahmad, F.** (1991) Long-term temperature and salinity variations near Jeddah in relation to certain meteorological factors over the Red Sea, *JKAU: Mar. Sci*., **2**: 19-29.

Walton, C.C., Pichel, W.G., Sapper, J.F. and **May, D.A.** (1998) The Development and Operational Application of Nonlinear Algorithms for the Measurement of Sea Surface Temperatures with the NOAA Polar-Orbiting Environmental Satellites, *J. Geophys. Res*., **103**(27): 999-28,012.

Wassef, R.K., Gerges, M.A. and **Soliman, G.F.** (1983) Wind driven circulation in the Red Sea as a homogeneous basin, *Bulletin of the Institute of Oceanography and Fisheries*, Cairo, 9.

الأنماط الزمانية والمكانية لدرجة حرارة المياه السطحية المستشعرة عن بعد في شمال البحر الأحمر

عبدالله محمد الصبحي و موسى محمد الأقصم

كلية علوم البحار، جامعة الملك عبدالعزيز

جدة – المملكة العربية السعودية

amalsubhi@kau.edu.sa

المستخلص. أظهرت دراسة المعدلات الشهرية لدرجة حرارة البحر الأحمر السطحية للفترة بين يناير ١٩٩٦م إلى ديسمبر ٢٠٠٣م المقاسة بالأقمار الصناعية في النصف الشمالي للبحر الأحمر، بأن درجة حرارة البحر السطحية، تزداد من الشمال إلى الجنوب، ومن الغرب إلى الشرق، ودرجة الحرارة الأعلى، في المنطقة الجنوبية الشرقية، والمنطقة الشرقية على الجانب السعودي، بينما تكون منخفضة على الجانب الأفريقي. من ناحية أخرى، أظهر نموذج انحدار متعدد لحساب درجة حرارة البحر السطحية، بأنها مرتبطة بتغيرات درجة الحرارة الجوية وسرعة الرياح، والتدفق الناتج عن البخر. كما أوضح التحليل الطيفي أن الدورة السنوية هي المهيمنة بالنسبة لتغير درجة الحرارة السطحية في شمال البحر الأحمر، بينما بينت مركبة الدورة بين السنوية درجات حرارة مرتفعة للفترة (١٩٩٧ – ١٩٩٩م) قد تكون نتيجة إلى تأثير ظاهرة إلنينو، ودرجات حرارة منخفضة أثناء الفترة (٢٠٠٠ – ٢٠٠٣م) قد تكون بسبب ظاهرة لآنينا أو نتيجة لدورة ١١ سنه الناتجة عن نشاط البقع الشمسية ، والذي يحتاج إثباته إلى مزيد من البحث والدراسه.